ORNL/SPR-2019/1071

Resolution Capabilities for Measurement of Fuel Swelling Using Tomography

Nuclear Technology Research and Development

Prepared for
US Department of Energy
Advanced Fuels Campaign
M.D. Richardson, G.W. Helmreich,
A.M. Raftery, A.T. Nelson
Oak Ridge National Laboratory
February 1, 2019
M4FT-19OR020201062

SUMMARY

The miniature fuel (MiniFuel) irradiation experimental design at Oak Ridge National Laboratory (ORNL) enables irradiation testing of small fuel specimens in the High Flux Isotope Reactor (HFIR) in support of the Advanced Fuels Campaign (AFC). The first set of irradiated MiniFuel specimens will be available for post-irradiation examination this year. X-ray computed tomography (XCT) has been established as a viable method for determining the post-irradiation volume of the specimens and the corresponding swelling due to irradiation. The work described herein explored the resolution capabilities in using XCT to determine the volume of representative MiniFuel geometries. Strategies for optimization of the parameters used during the measurement and the uncertainty of the method according to specimen geometry are reported.

CONTENTS

This page is intentionally left blank.

FIGURES

TABLES

ACRONYMS

ORNL	Oak Ridge National Laboratory
AFC	Advanced Fuels Campaign
AGR	Advanced Gas Reactor
HFIR	High Flux Isotope Reactor
PIE	Post-Irradiation Examination
TRISO	Tristructural Isotropic
XCT	X-ray Computed Tomography

This page is intentionally left blank.

ACKNOWLEDGMENTS

This work was supported by the Advanced Fuels Campaign of the US Department of Energy Office of Nuclear Energy. We would like to acknowledge Randy Parten for manufacturing the zirconia and tungsten specimens that were used as material standards in the report.

This page is intentionally left blank.

RESOLUTION CAPABILITIES FOR MEASUREMENT OF FUEL SWELLING USING TOMOGRAPHY

1. INTRODUCTION

The objective of the Miniature Fuel (MiniFuel) project at Oak Ridge National Laboratory (ORNL) is to irradiate small fuel specimens to obtain separate effects and screening data on various candidate and existing nuclear fuel types. The current strategy is for the design to be used initially for separate effects testing of UN, UO_2, and U_3Si_2 in support of the Advanced Fuels Campaign (AFC) [1]. Two MiniFuel targets containing UN and tristructural isotropic (TRISO) kernel specimens were inserted into the High Flux Isotope Reactor (HFIR) in the summer of 2018 [2]. The first target will be ready for disassembly and post-irradiation examination (PIE) in 2019. The methodology to be used for PIE of the fuel specimens has been established, including procedures for disassembly and measurement of the fission gas release and swelling [3].

X-ray computed tomography (XCT) was the main method demonstrated for obtaining the fuel swelling measurement after irradiation. During irradiation, the fuel will expand in volume due to the creation of gaseous and solid fission products. The amount of fuel swelling is considered an important measure of the fuel's performance since it is a direct indicator of fission product production and material behavior. Fuel swelling can be determined by measuring the fuel volume pre- and post-irradiation. XCT has been used as part of the Advanced Gas Reactor (AGR) program and has proven to be a valuable characterization tool for unirradiated and irradiated fuel kernels [4].

The use of XCT to determine the volume of samples representative of the MiniFuel kernel geometries has been explored in a previous report [3]. The purpose of this report is to analyze expansion of the use of XCT to include volume determination of disk and compact geometries. In addition, this work includes optimization of the XCT method to enable greater specimen throughput without compromising measurement accuracy.

2. MINIFUEL DESIGN AND SWELLING MEASUREMENT

The MiniFuel design has been described thoroughly in previous work [5–7]. The main components are a basket, target, and sub-capsule (Figure 1). Each target holds six sealed titanium sub-capsules. Each sub-capsule contains a molybdenum tube, a piece of SiC thermometry, a molybdenum cup, and the fuel specimens. The molybdenum cup holds the fuel specimens and is easily adapted to hold various fuel geometries, including a range of kernel sizes and disks. Figure 2 shows the configurations currently available for use in testing fuel specimens.

While the flexibility in fuel design creates a unique opportunity for tailored test matrices, the small fuel size of each geometry also presents challenges in determining the fuel volume. Many methods used for determining fuel volume have accuracies dependent upon specimen size [8]. Methods with the highest level of accuracy for small volumes often require the use of toxic substances [9,10] or are complex in nature [11,12]. XCT was chosen as the primary method to use when determining volume for the MiniFuel project because it is non-destructive, and it uses an established capability for performing the measurements of interest.

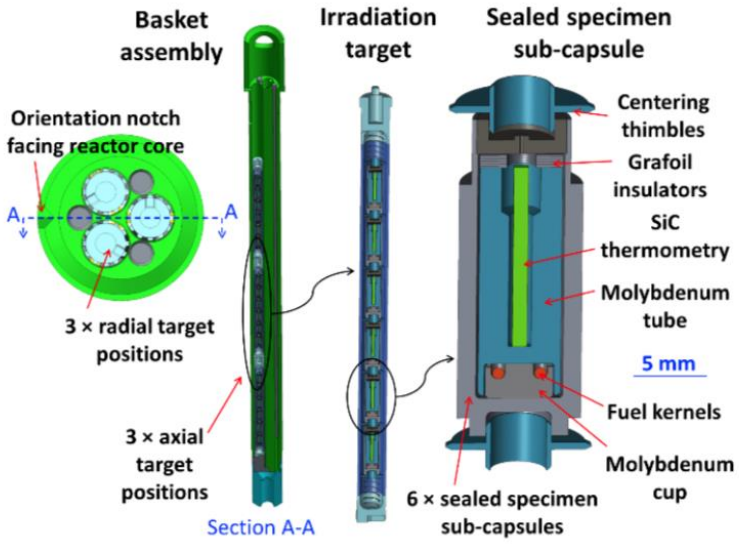

Figure 1. Schematic of the MiniFuel basket, target, and sub-capsule design [7].

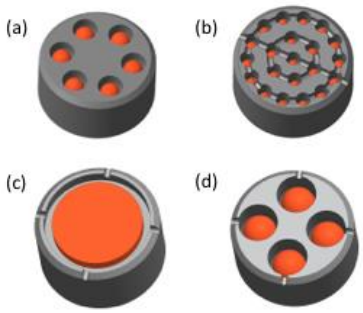

Figure 2. Molybdenum disk layout with (a) six 800 µm UN kernels, (b) twenty-one 425 µm UC kernels, (c) one 3 mm disk, and (d) four 1 mm TRISO particles [3].

3. XCT METHOD DESCRIPTION

Volume determination using XCT involves two steps: sample imaging and image segmentation. Samples were imaged using the Xradia MicroXCT-400 shown in Figure 3. This instrument collects a series of radiographs, which are two-dimensional projections of the three-dimensional sample, at a span of rotational angles. By using a span of at least 180 degrees of sample rotation, these radiographs can be mathematically combined to reconstruct a three-dimensional image of the sample, with the brightness being proportional to the x-ray absorbance in each region [3].

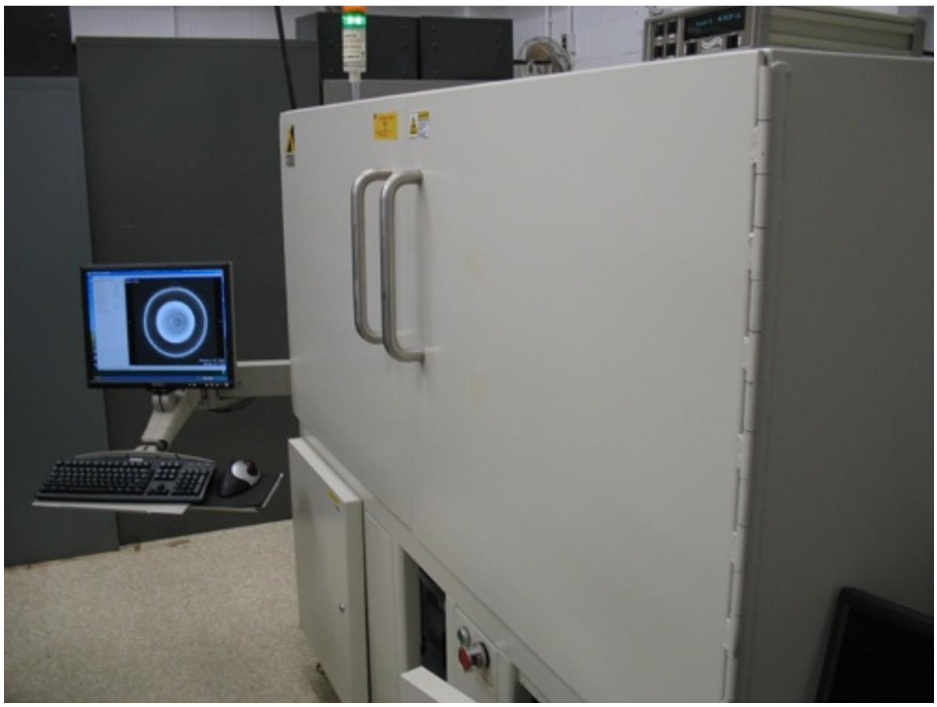

Figure 3. Xradia tomography system outfitted for use with radioactive materials [4].

Once reconstructed, three-dimensional intensity images were entered into custom MATLAB software designed to automate the image segmentation process. As a preliminary step, filtering and morphological operations were performed to reduce image noise and to enhance the sharpness of edges between materials. Initial segmentation thresholds were estimated using Otsu's method [13] and were then verified by the user, allowing for interactive modification of threshold values if necessary. After user verification, the three-dimensional image was segmented into groupings of voxels (three-dimensional pixels) of the same material. This initial segmentation was then improved using a series of morphological operations based on the known cylindrical geometry of the material. Combining the segmented image with the known image resolution produced quantitative measurements of the sample geometry such as volume, radius, and height. Figure 4 below shows the various steps involved in using the software, starting with the initial image (top left), adjusting the contrast of the image (top right), finding an initial threshold (bottom left), and determining the final segmentation of the image (bottom right). For the initial segmentation, a high threshold value was used to capture the bright ring around the edge of the disk, resulting in the red coloration seen in the bottom left image. The ring was then filled in to achieve the final segmentation, resulting in the bottom right image.

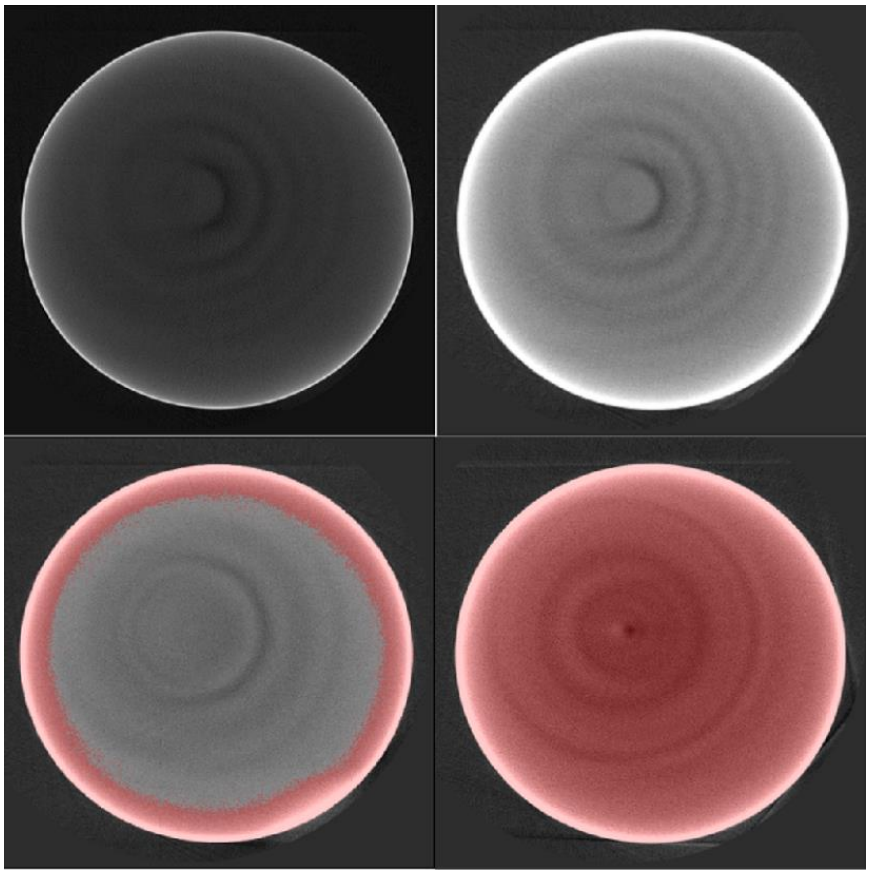

Figure 4: Cross section of tungsten disk showing the original image (top left), adjusted image (top right), initial thresholding (bottom left), and final segmentation (bottom right). The red ring in the bottom left captured the bright ring around the edge of the disk before being filled in in the bottom right image for the final segmentation of the disk.

4. UNCERTAINTY ANALYSIS

Determination of the uncertainty for XCT volumes is complex. The primary source of uncertainty in the measured XCT volume is the position of the boundary in the segmentation between the sample and its surroundings. The uncertainty in this position may be estimated based on a plot of the image brightness at the boundary. The brightness can be affected by sample geometry and the specific imaging conditions used to perform the measurement. High quality XCT imaging to resolve interior features such as layer defects in TRISO particles typically requires 3,200 frames taken with a 15-second exposure, resulting in an imaging time of approximately one full day. For the more straightforward application of determining overall sample volume and geometry, fewer frames and a lower exposure time may result in higher sample throughput without sacrificing accuracy.

4.1 IMAGING CONDITIONS

In order to check the effect of imaging conditions on the image brightness at the boundary, four imaging conditions were tested. The conditions were tested using samples with approximately the expected geometry and x-ray absorption of MiniFuel specimens. Tungsten disks were used as a surrogate for metallic uranium, and zirconia disks were used as a surrogate for uranium ceramics. The disks were approximately 3 mm in diameter with a height of 0.3 mm. The XCT beam power was set to 90 kV for the voltage and 88 µA for the current because of the high Z of the materials used.

Figure 5 shows the image brightness along radial lines from the center of the tungsten disk to the outside for each of the four imaging conditions tested. The brightness near the edge of the disk is significantly greater than inside due to the low x-ray transmission of the material. At the boundary between the sample and the surroundings, the brightness shifts rapidly from the high-intensity edge downward. The imaging condition with 800 frames and 8 seconds per frame gives the most drastic change in brightness and is therefore associated with the lowest uncertainty. However, there is little change between these conditions and those with 400 frames and 8 seconds per frame, meaning that time can be saved without compromising accuracy in the method.

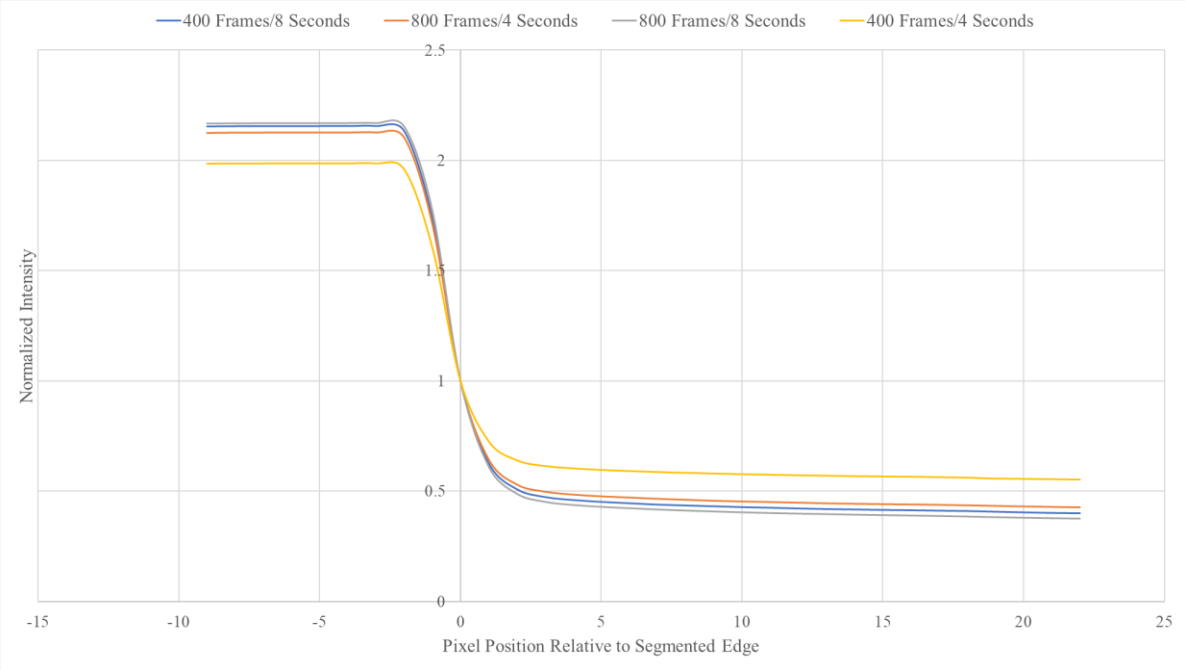

Figure 5: Normalized intensity curves along radial lines for each case used with the tungsten disk.

4.2 SPECIMEN GEOMETRY

Determining the boundary of the specimen is done by analyzing the change in brightness across the edge of the specimen. The same tungsten and zirconia disk (3 mm x 0.3 mm) specimens were used to determine the effects of the specimen shape on the uncertainty in the method. Figure 6 shows a graph of brightness across the radial dimension of the tungsten specimen for the parameters of 800 frames and 8 seconds of exposure. The y-axis in Figure 6 marks the boundary found by the existing MATLAB image

segmentation algorithm. As expected, the boundary is near the center of the intensity curves. The uncertainty for each case was estimated by finding the pixel range that captured ±25% of the total range of the intensity change across the curve. This was arbitrarily selected by looking at the image and choosing a reasonable range. This process was completed for the radial, top, and bottom boundaries for each disk under each imaging condition, and the uncertainties in each boundary were then propagated into the total volume uncertainty. This was done by using a linear fit of the position to intensity to find the pixel values corresponding to the ±25% range of intensities around the curve center. Taking half of the distance from these pixel values and multiplying by the scale allowed for the uncertainty to be calculated in micrometers instead of pixels.

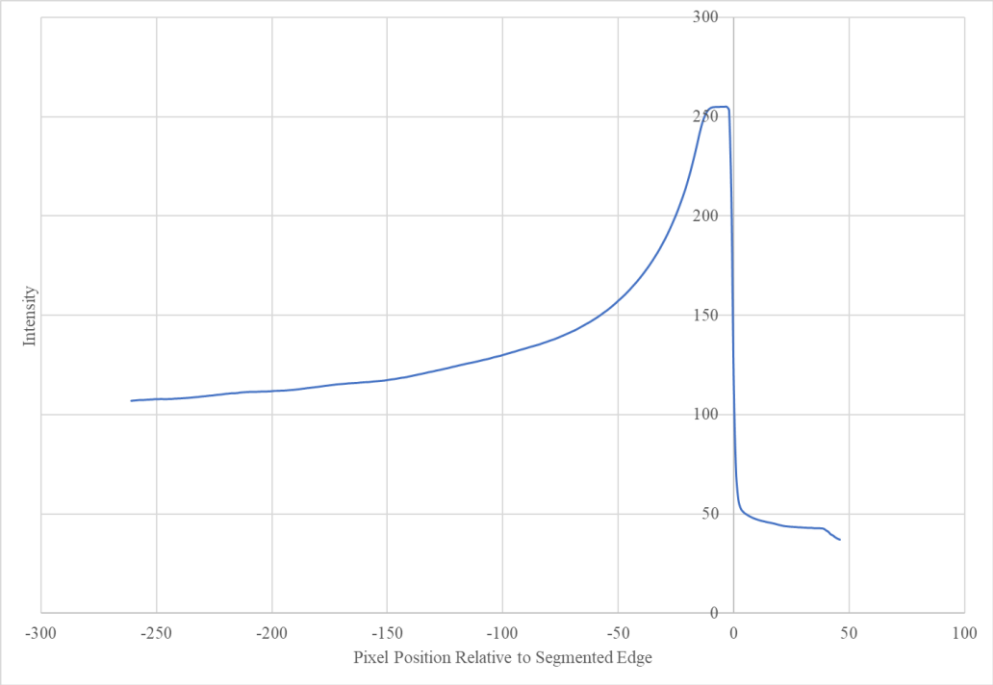

Figure 6: Intensity curve along radial lines for tungsten disk measured at 800 frames and 8 seconds of exposure time.

Figures 7 and 8 show the normalized radial, top, and bottom boundaries for the tungsten and zirconia disks imaged at 800 frames and at 8 seconds of exposure time, respectively. These graphs show the same result for the two different materials, which is that the change in the brightness is much less drastic for the height of the disk compared to the diameter. Therefore, the primary contribution to XCT volume uncertainty (~70%) comes from the uncertainty at the top and the bottom of the disk, not the radial edge. This can be seen in Table 1 for both materials at different measurement parameters. The reasons for this are two-fold. First, edge effects caused by incomplete x-ray penetration of high-Z materials result in a sharp increase in brightness at the radial edge, as shown in Figures 5, 6, 7, and 8. This edge effect results in a sharp boundary with little associated uncertainty. Second, the sample geometry of a wide, short disk results in a much greater impact per unit of absolute uncertainty on the relative uncertainty in the height.

Table 1: Uncertainty contribution of uncertainty for radius and height for both materials.

Material (Frames/Exposure)	Radius Uncertainty (µm)	Total Height Uncertainty (µm)	Height Uncertainty Contribution (%)
Tungsten (400/8)	3.412	8.663	71.74
Tungsten (800/4)	3.404	8.734	71.96
Tungsten (800/8)	3.317	8.499	71.93
Zirconia (400/8)	2.903	8.554	74.66
Zirconia (800/4)	2.663	7.917	74.83
Zirconia (800/8)	2.579	7.952	75.51

These factors suggest two methods to reduce uncertainty in XCT volume measurements. First, rotating the sample 90 degrees to transfer the beneficial edge effect to the top and bottom of the sample may reduce the overall uncertainty due to the greater impact of uncertainty in the top and bottom on the total volume uncertainty. Second, the sample geometry may be optimized to reduce uncertainty. Spherical samples and cylinders with heights approximately equal to their diameters will have significantly reduced uncertainty based on the results shown here.

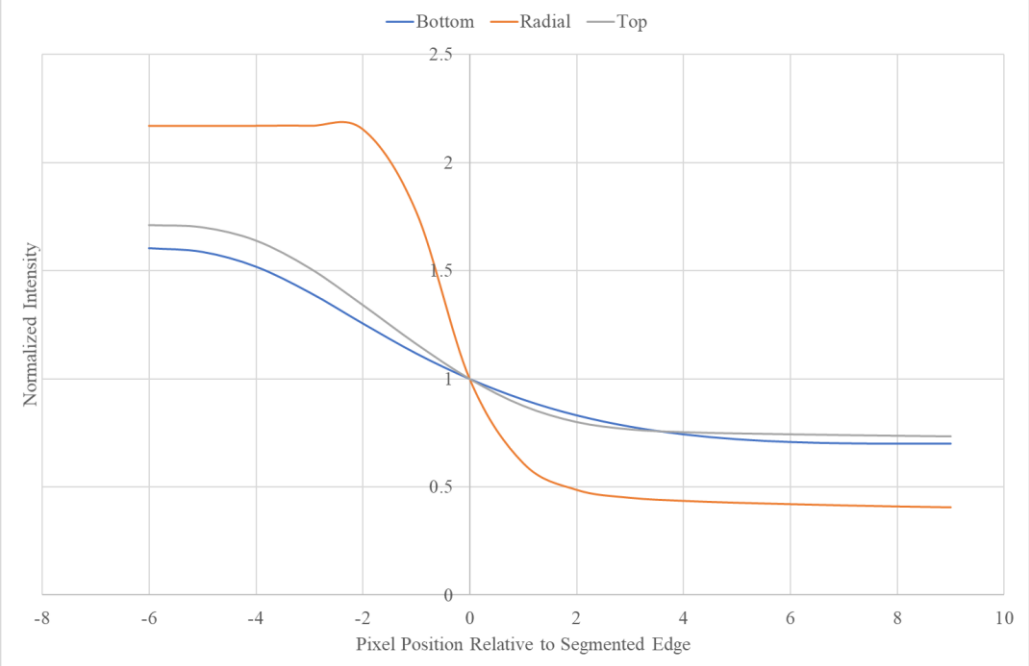

Figure 7: Normalized intensity curves for the radial, bottom, and top boundaries for the tungsten disk measured at 800 frames and 8 seconds of exposure time.

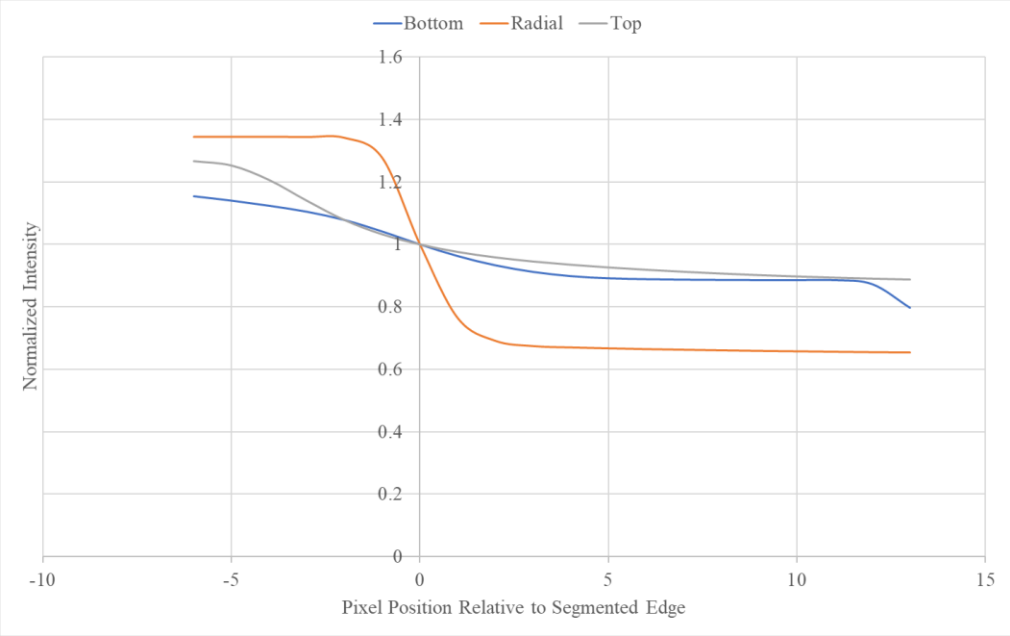

Figure 8: Normalized intensity curves for the radial, bottom, and top boundaries for the zirconia disk measured at 800 frames and 8 seconds of exposure time.

4.3 TOTAL VOLUME UNCERTAINTY

The nominal volume of the tungsten and zirconia disks were determined using Archimedes' method and a microbalance. Larger pieces of material cut from the same rod were measured for density using Archimedes, and the mass of the specimens was measured using a WXTP26 microbalance. The calculated volume was then compared to the volume measured by segmenting the XCT images acquired under varying conditions to determine their impact on accuracy. The results from this test matrix are given in Table 2. Uncertainty values for the nominal volumes in Table 2 were determined based on the propagated uncertainties from the sample's mass and density obtained using Archimedes' method.

These results show that the volume determined using Archimedes and tomography match closely. As expected, the uncertainty as determined from the curvature of the image brightness at the sample edge was reduced with increasing exposure time and number of frames in the XCT images. Both of these changes increased the image quality at the sample's edge, resulting in a sharper transition and reduced uncertainty at the cost of increased total imaging time. The resulting uncertainties for the most precise conditions (i.e., most frames and longest exposure time) are 2.85% for tungsten and 2.64% for zirconia.

Table 2. Results from varying frames and exposure rate for fuel surrogate materials.

Material	Frames	Exposure (s)	Nominal Volume (mm^3)	XCT Volume (mm^3)	Relative Uncertainty (%)
Tungsten	400	4	2.718 ± 0.007	2.608 ± 0.087	3.33
Tungsten	400	8	2.718 ± 0.007	2.652 ± 0.077	2.90
Tungsten	800	4	2.718 ± 0.007	2.654 ± 0.078	2.92
Tungsten	800	8	2.718 ± 0.007	2.666 ± 0.076	2.85
Zirconia	400	4	2.449 ± 0.018	2.351 ± 0.073	3.01
Zirconia	400	8	2.449 ± 0.018	2.377 ± 0.068	2.86
Zirconia	800	4	2.449 ± 0.018	2.383 ± 0.063	2.65
Zirconia	800	8	2.449 ± 0.018	2.385 ± 0.063	2.64

5. MINIFUEL SWELLING RESOLUTION

The ability to determine the swelling for representative MiniFuel specimens was determined using the previous analysis on disk geometry. The minimum uncertainty in the XCT volume measurement (zirconia at 800 frames and 8 seconds) was used to determine the uncertainty in the swelling measurement. This was done using the equation for propagation of uncertainty,

$$\sigma_{\frac{\Delta V}{V}} = \sqrt{\frac{\sigma_{V_1}^2+\sigma_{V_2}^2}{(V_2-V_1)^2} + \frac{\sigma_{V_1}^2}{V_1^2}} \quad (1)$$

where V_1 is the pre-irradiation volume measurement, V_2 is the post-irradiation volume measurement, σ_1 is the XCT uncertainty in the pre-irradiation volume measurement, and σ_2 is the XCT uncertainty in the post-irradiation volume measurement. Figure 9 shows a graph of representative swelling values for uranium nitride fuel [14] and the window of maximum and minimum error that would be associated with the XCT method. Figure 10 shows a similar graph for uranium dioxide representative values [15]. The irradiation conditions for each reference swelling condition are summarized in Table 3. It is clear from these plots that the methods of XCT will be sufficient to measure the swelling of intermediate- to high-swelling materials, even at low (~5 MWd/kgU) burnup conditions. These graphs are specifically for the MiniFuel geometry disk (3 mm diameter x 0.3 mm height), and they are expected to be more favorable for kernel and compact geometries for reasons outlined in Section 4.2.

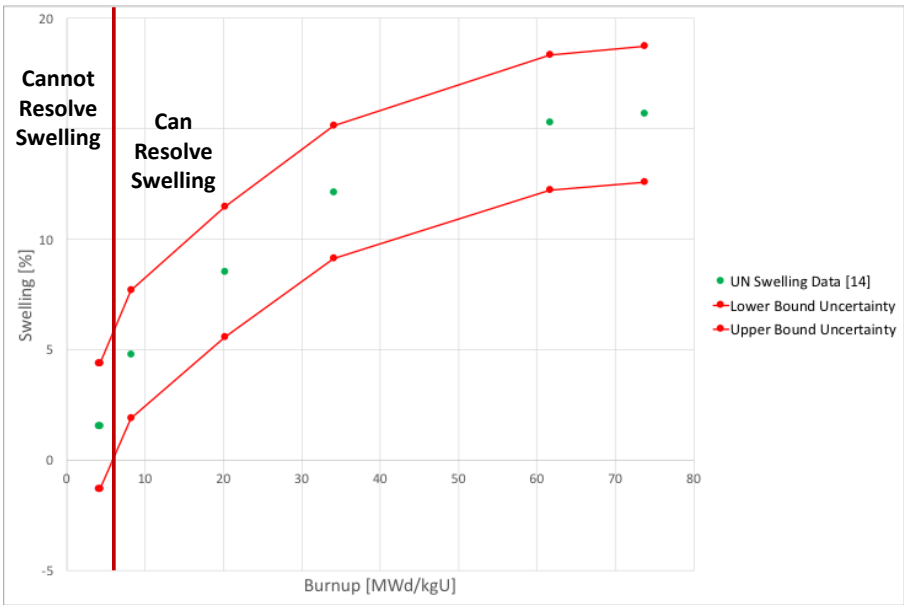

Figure 9. Graph of burnup vs. swelling of uranium nitride [14], highlighting the favorable resolution capabilities for determining the swelling of intermediate to high-swelling materials using tomography.

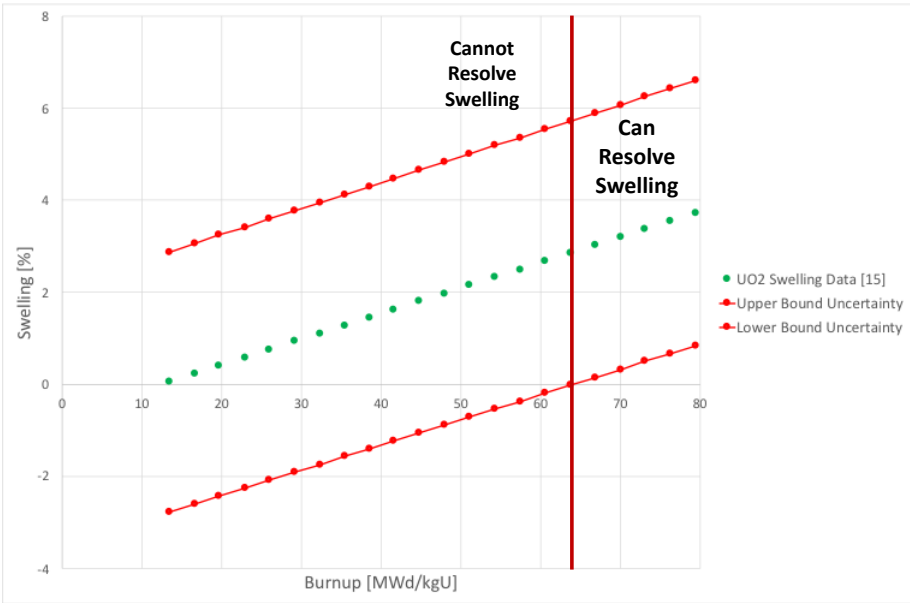

Figure 10. Graph of burnup vs. swelling of uranium dioxide [15], highlighting the minimal resolution capabilities for determining the swelling of low-swelling materials using tomography.

Table 3. Irradiation conditions for reference swelling values used in Figure 9 and Figure 10.

Fuel	Fuel Density	Cladding	Temperature	Reference
UN	87% TD	Nb-Zr	977 - 1277°C	[14]
UO_2	95% TD	M5	800 - 900°C	[15]

6. SUMMARY AND FUTURE WORK

This work primarily aimed at furthering the development of XCT methods used to determine the volume of irradiated specimens. The XCT-acquired pre- and post-irradiation volume measurement will be used to determine fuel specimen swelling as part of the MiniFuel project at ORNL.

Two main parameters—frame count and exposure time—were varied to test the effects on method uncertainty. The optimization of these values ensures that the highest level of accuracy can be achieved while also maximizing the potential throughput of specimens. The effect of specimen geometry on the uncertainty has also been tested, and it has been shown that small disk specimens likely have the largest uncertainty due to the difficulty in the method for determining the small specimen's height (~0.3mm). It is speculated that compact specimens with greater heights and spherical (kernel) specimens will inherently have lower uncertainty values. The use of helium pycnometry is also currently under development to compliment the use of XCT. Therefore, the chosen method will likely depend on the specific specimen geometry and the achievable uncertainty associated with each method.

The methods developed in this report will be used to analyze the first set of MiniFuel specimens, which will be ready for PIE this year. In addition, these methods will be used to make pre-irradiation and post-irradiation volume measurements on future disk and compact specimens planned as part of the MiniFuel project.

7. REFERENCES

[1] Nelson, A., Petrie, C., Coordinated MiniFuel Irradiation Test Plan for Ceramic Fuels, Los Alamos National Laboratory and Oak Ridge National Laboratory, November 2017.

[2] Petrie, C.M., Burns, J.R., Morris, R.N., Smith, K.R., Le Coq, A.G., Terrani, K.A., Irradiation of Miniature Fuel Specimens in the High Flux Isotope Reactor, ORNL/SR-2018/874, Oak Ridge National Laboratory, June 2018.

[3] Raftery, A., Morris, R., Smith, K., Helmreich, G., Petrie, C., Terrani, K., Nelson, A., Development of a Characterization Methodology for Post-irradiation Examination of Miniature Fuel Specimens, ORNL/SPR-2018/918, Oak Ridge National Laboratory, August 2018.

[4] Hunn, J., Morris, R., Baldwin, C., Montgomery, F., Chinthaka Silva, G., Gerczak, T., AGR-1 Irradiated Compact 4-4-2 PIE Report: Evaluation of As-Irradiated Fuel Performance with Leach Burn Leach, IMGA, Materialography, and X-ray Tomography, ORNL/TM-2013/236, Oak Ridge National Laboratory, September 2013.

[5] Petrie, C., M., Burns, J., Morris, R., Terrani, K., Miniature Fuel Irradiations in the High Flux Isotope Reactor. Proceedings of the Enlarged Halden Programme Group Meeting, Lillehammer, Norway, 2017.

[6] Petrie, C., Burns, J., Morris, R., Terrani, K., Small-scale fuel irradiation testing in the high flux isotope reactor, Proceedings of the 2017 Water Reactor Fuel Performance Meeting, Jeju Island, Korea, 2017.

[7] Petrie, C., Burns, J., Morris, R., Terrani, K., Accelerated Irradiation Testing of Miniature Fuel Specimens, Nuclear Fuels and Structural Materials for the Next Generation Nuclear Reactors in ANS Annual Meeting, Philadelphia, PA, 2018.

[8] Blank, E., Willard, M., Micro-density determination of solids and liquids, Journal of Chemical Education, 10 (1933) 109-112.

[9] Yamagishi, S., Takahashi, Y., Shiba, K., An accurate method for determining the small volumes of granular solids by mercury pycnometry, Journal of Physics E: Scientific Instruments, 17 (1984) 339-341.

[10] Fascia, J.R., Johnston, W.V., A Micropycnometer for measuring densities of powdered materials, Knolls Atomic Laboratory, November 1961.

[11] Neumerzhitskii, V.T., Toropin, S.P., Chernikova, O.L., Volume and Density Measuring Device for shapeless, loose-powder and porous bodies, Izmeritel'naya Teknika, 1 (1988) 21–22.

[12] Franklin, A.D., Spal, R., A method for precision comparison of the densities of small specimens, The Review of Scientific Instruments, 42 (1971) 1827–1833.

[13] Kittler, J., Illingworth, J., On threshold selection using clustering criteria, IEEE Transactions on Systems, Man, and Cybernetics, 15 (1985) 652–655.

[14] Matthews, B., Irradiation Performance of Nitride Fuels in Conference on Space Nuclear Power and Propulsion Technologies, Los Alamos National Laboratory, September 1993.

[15] Noirot, J., Aubrun, I., Desgranges, L., Hanifi, J., Lamontagne, J., Pasquet, B., Valot, C., Blanpain, P., Cognon, H., High burnup changes in UO_2 fuels irradiated up to 83 GWd/T in M5 claddings, Nuclear Engineering and Technology, 41 (2009) 155-162.